KARYA ILHAM PUBLISHING
CONNECTING MINDS, BRIDGING IDEAS, INSPIRING READERS

Future Energy and Environment Letters

Journal homepage:
https://karyailham.com.my/index.php/feel
ISSN: 3083-8940

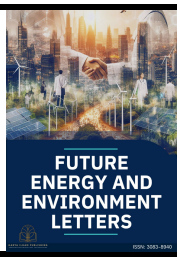

The Effect of Glutaraldehyde Crosslinking on the Performance of Hybrid PVA-Chitosan-Polyaniline Hydrogel for Solar Vapor Generation

Syazwani Mohd Zaki[1,*], Flora Serati[2], Ahmad Akid Zulkifli[1]

[1] Department of Manufacturing and Materials Engineering, Kulliyah of Engineering, International Islamic University Malaysia, PO Box, 50728 Kuala Lumpur, Malaysia
[2] Department of Electrical and Computer Engineering, Kulliyah of Engineering, International Islamic University Malaysia, PO Box, 50728 Kuala Lumpur, Malaysia

ARTICLE INFO

Article history:
Received 10 October 2025
Received in revised form 15 October 2025
Accepted 14 November 2025
Available online 7 December 2025

ABSTRACT

Solar Vapor Generation (SVG) stands out as a potent solution among other options, harnessing abundant solar energy to generate clean water through an evaporation process similar to the natural water cycle. Crosslinkers are fundamental components in the design and functionality of polymer hydrogel for SVG applications. The primary role of a crosslinker is to establish the three-dimensional network structure of hydrogels, which directly governs mechanical properties, water transport efficiency, and overall performance in solar-driven evaporation processes. The optimisation of crosslinkers leads to a more efficient SVG system. In this work, hybrid hydrogels of polyvinyl alcohol-chitosan (PVA-CS) and polyaniline (PANI) with varying concentrations of Glutaraldehyde (GA) were studied to evaluate the hydrogel's rigidity and performance in facilitating the SVG system. Herein, we report the preparation of PVA-CS hydrogels with the addition of polyaniline (PANi) at different glutaraldehyde (GA) concentrations. PVA-CS hydrogels without PANi are denoted as PVA-CS-0.42 wt.% GA and PVA-CS-0.48 wt.% GA, whereas PVA-CS hydrogels with PANi are denoted as PVA-CS-0.42 wt.% GA-PANi and PVA-CS-0.48 wt.% GA-PANi. The PVA-CS hydrogel with PANi copolymers was prepared by solution polymerisation to incorporate PANi into the hydrogel network structure. The storage modulus of the PVA-CS hydrogels for all systems was determined by rheology. The storage modulus (G') of PVA-CS-0.48 wt.% GA-PANi depicted the highest value of 2948 Pa compared to PVA-CS-0.42 wt.% GA-PANi, which depicted the G' value of 2362 Pa. The Tan δ value of PVA-Chitosan-0.48 wt.% GA-PANi was 0.05, indicating elastic behaviour. From FTIR analysis, an absorption band was observed between 3600 and 3000 cm^{-1}, attributed to the O-H and N-H groups of PVA and PANi, and was also evident in the PVA-CS hydrogel with the highest GA concentration, 0.48 wt.%. The microporous structure of PVA-Chitosan hydrogel with

* *Corresponding Author*
E-mail address: syazwani_mohdzaki@iium.edu.my

https://doi.org/10.37934/feel.5.1.2030

PANi distribution increases with higher concentration of GA, which demonstrates that the degree of cross-linking of PANi gives a more rigid structure of porous hydrogel. Therefore, it is expected that this hydrogel will scatter natural sunlight across its surface, efficiently converting light to heat at the evaporating surface, thereby supporting an efficient SVG design platform.

Keywords:
Polymer Hydrogel; Solar Vapor Generation; Polyaniline

1. Introduction

Water conservation is a critical global priority, given that only 3% of the Earth's water is freshwater, with a mere 0.5% readily accessible for human consumption [1]. Rapid population growth and increasing pressure on finite freshwater resources necessitate urgent conservation measures to ensure the sustainable availability of freshwater for future generations. Effective water preservation mitigates the adverse effects of drought, reduces the economic costs associated with water scarcity, and minimizes the potential for geopolitical conflicts over dwindling water supplies. Solar vapor generation (SVG) stands out as a promising solution among various options, harnessing abundant solar energy to produce clean water through an evaporation process like the natural water cycle [2]. The optimal performance of SVG systems is governed by two critical elements: a solar absorber that converts solar radiation into heat and a substrate material that ensures an effective water supply while suppressing heat loss [3]. Polymer hydrogels have emerged as highly promising materials for SVG due to their exceptional water absorption, retention, and transport capabilities [4]. Among the various strategies to enhance their performance, the incorporation of glutaraldehyde (GA) as a crosslinker has been shown to significantly improve their structural integrity and efficiency in solar-driven water evaporation applications. The chemical cross-linking ability of GA reinforces the hydrogel's mechanical properties and stability, which are critical for sustaining high evaporation rates under prolonged solar exposure [5]. One of the key advantages of polymer hydrogels in SVG is their high photothermal conversion efficiency. Conjugated polymer hydrogels exhibit superior light-to-heat conversion capabilities, enabling efficient solar-driven water evaporation. This efficiency is further enhanced by the hydrogel's ability to localize heat and facilitate rapid water transport, thereby minimizing energy loss [6]. Additionally, the interconnected porous structure of hydrogels plays a crucial role in optimizing water mass transportation and light absorption. For instance, PVA-chitosan with polyaniline (PANi) hydrogel was synthesized by copolymerizing PVA and chitosan with PANi through solution polymerization, enhancing its light absorption properties. Its microporous structure, influenced by the PVA concentration, becomes more rigid at higher cross-linking densities, thereby improving both dye adsorption and water evaporation. The PVA-CS/PANi with the highest concentrations reportedly achieves 69.8% SVG efficiency under 1 sun, demonstrating strong light-to-heat conversion [7]. This makes it promising for applications in water purification and desalination. Further, polyelectrolyte hydrogels such as PVA/carbon nanotubes-co-poly(acrylic acid)-co-poly dimethyl diallyl ammonium chloride (PVA/CNTs-co-PAA-co-PDADMAC) (PADM) polyelectrolyte hydrogels, which feature a well-designed porous network, have demonstrated an impressive evaporation rate of 3.58 kg m^{-2} h^{-1}, attributed to their controllable cross-linking degree and efficient water pathways [8]. Another notable benefit of polymer hydrogels is their exceptional salt tolerance, which ensures stable performance even in high-salinity environments. This property is particularly advantageous for desalination applications, where salt accumulation often poses a challenge to long-term efficiency. Studies have shown that polymer hydrogels can maintain high evaporation rates in concentrated brine, highlighting their robustness for practical use [8, 9]. Comparatively, other hydrogel systems, such as those incorporating carbon nanoparticles or MXene nanosheets and silver nanoparticles (AgMXene) nanocomposites, have shown varying evaporation rates and efficiencies.

For instance, a chitosan/PVA hydrogel with carbon nanoparticles achieved an evaporation rate of 2.28 kg m^{-2} h^{-1}, while a chitosan-based hydrogel with AgMXene nanocomposites reached an evaporation efficiency of 93% [10, 11].

Crosslinkers are essential in determining the design and performance of polymer hydrogels, especially for solar vapor generation (SVG) applications. They form the three-dimensional (3D) polymeric network that governs the hydrogel's mechanical strength, water transport, and overall evaporation efficiency [12]. By selecting and optimizing suitable crosslinkers, researchers can tailor the structural integrity, porosity, and hydrophilicity of hydrogels to achieve more effective solar-driven evaporation. The mechanical reinforcement provided by crosslinkers is one of their most significant contributions. For instance, spherical polymer brush crosslinkers incorporated into poly(acrylic acid) (PAA) hydrogels have been reported to impart exceptional stretchability and toughness, maintaining durability under mechanical stress during solar evaporation [13]. Likewise, the combination of dynamic and permanent cross-links in photo-cross-linked poly(ethylene oxide)-based hydrogels enhances both elasticity and fracture resistance, ensuring robust operation during repeated hydration dehydration cycles [14]. These mechanical improvements are vital for ensuring long-term stability in SVG systems, which are continuously exposed to water and fluctuating temperatures. Beyond mechanical strength, crosslinkers strongly influence porosity and water transport behavior. A well-controlled degree of crosslinking, as in PADM polyelectrolyte hydrogels, promotes the formation of interconnected porous channels that facilitate efficient water flow and vapor diffusion [8]. Similarly, adjusting the crosslinker concentration in sponge-like composite hydrogels allows for a balance between water delivery rate and heat localization, thereby improving overall evaporation efficiency [5].

Crosslinkers also play a critical role in photothermal performance. Conjugated polymer hydrogels exhibit a high light-to-heat conversion capability, thereby reducing the energy required for water evaporation [6]. Moreover, gradient-charged hydrogels with tailored crosslinking gradients can enhance solar steam generation by establishing osmotic pressure differences that promote efficient water and ion transport during desalination [9]. These findings collectively highlight the central role of crosslinker chemistry in controlling energy efficiency and functional stability in solar-driven evaporation systems. Optimized crosslinking also contributes to salt resistance and operational durability. For example, PADM hydrogels with controlled cross-linking density maintain stable evaporation rates and exhibit resistance to salt crystallization even under prolonged use [8]. Likewise, azo-crosslinked double-network hydrogels increase mechanoradical concentration, expanding their photothermal and structural functionality for long-term SVG applications [15]. Among various crosslinkers, glutaraldehyde (GA) has emerged as a particularly effective and versatile agent. Its bifunctional aldehyde groups enable covalent bonding with hydroxyl and amino functionalities in polymer chains, forming stable linkages that reinforce the hydrogel's network structure [16]. This mechanism markedly enhances mechanical strength, thermal resistance, and chemical stability, making GA-crosslinked hydrogels suitable for challenging environments such as solar evaporation systems [17,18]. The stability imparted by GA ensures consistent performance under variations in temperature and pH, preventing structural degradation during repeated cycles [19,20]. Furthermore, GA crosslinking significantly improves the swelling capacity and porosity of hydrogels, both of which are crucial for maintaining water supply to the evaporating interface. Enhanced pore structure promotes rapid water transport, thereby increasing the evaporation rate [8,17,19]. These combined effects underscore GA's critical importance in advanced hydrogel design for SVG applications. However, its concentration must be optimized, as excessive crosslinking while strengthening the hydrogel can reduce porosity and restrict water mobility, ultimately lowering evaporation efficiency [21]. Most previous studies on polymer hydrogels for SVG have focused on maximizing evaporation

rates without systematically examining how crosslinker concentration influences mechanical stability and photothermal performance. Limited attention has been given to the optimization of glutaraldehyde (GA) as a crosslinker in hybrid PVA-CS/PANi systems. This study aims to address this gap by correlating GA concentration with the structural rigidity, solar absorption, and SVG efficiency of the PVA-CS/PANi hydrogel.

2. Methodology

2.1 Materials

Materials used for this experiment are 0.32 M aniline monomers, 0.08 M ammonium persulfate (APS), hydrochloric acid (HCl,1M), deionized water (DI), 0.3 mol of polyvinyl alcohol (PVA) powder, 0.44 mol% of chitosan (CS) powder, calcium carbonate powder ($CaCO_3$), glutaraldehyde [GA, 50 wt % in deionized water], 150 ml distilled water. The chemicals were purchased from Sigma-Aldrich and R& M Chemicals

2.2 Method

The water bath was heated to a constant temperature of 80°C. The PVA powder was gradually added to the heated deionized (DI) water. After that, $CaCO_3$ powder was added to the mixture. Subsequently, the solution was stirred for 2 hours. Afterwards, the chitosan powder gradually added to the solution and stirred for another 6 hours. After 6 hours, the solution was transferred to another beaker to cool down at room temperature and formed the milky-white PVA-CS solution. Subsequently, 1 M HCI was added to the solution, which turned clear and was left to settle for an additional 2 hours. Polyaniline (PANi) was incorporated into the hydrogel and was prepared for gelation with Glutaraldehyde (GA) [50 wt.% in DI water] at concentrations ranging from 0.42 wt.% to 0.48 wt.%. 3 ml of the hydrogel solution was used, and GA was added. The gelation process was left to occur 24 hours

3. Results

3.1 FTIR analysis for PVA-CS and PVA-CS/PANi hydrogels

This section discusses the results obtained FTIR analysis of the study. The chemical structure of the PVA-CS hydrogels was assessed by FTIR spectrometry. FTIR spectra show the characteristics of the PVA-CS hydrogel, indicating the presence of crosslinking interactions. Fig. 1 depicts the FTIR spectra of the PVA-CS gel and PVA-CS with PANi between 4000-500 cm^{-1} to between 4000-500 cm^{-1}. A broad absorption band in the range of between 3650-3250 cm^{-1} that indicates hydrogen bonds in PVA-CS hydrogel. However, the sharp absorption band between 3632 cm^{-1} and 3571 cm^{-1} in the spectrum suggests the absence of hydrogen bonding, allowing the compound to contain an oxygen-containing group [22]. With the incorporation of PANI, the intensity of the -OH adsorption peak decreases, and the peak value shifts to lower wavenumber at 3260 cm^{-1} and 3262 cm^{-1} due to the overlap of the residual -OH groups in PVA and -NH groups in PANi [27]. Nevertheless, for PVA-CS hydrogels incorporating PANi, the absorption intensity decreased significantly in this area, especially at a GA concentration of 0.42 wt.%. An increase in the absorption band located at 1581 cm^{-1}, 1511 cm^{-1},1503 cm^{-1},1439 cm^{-1},1413 cm^{-1} indicates an increase in C=C and C=N bonds associated with quinoid rings and benzenoid rings, respectively, which also correlated to the stretching of PANi in the PVA matrix. The peak at 1650 cm^{-1} for both PVA-CS without PANi corresponds to C=N bending vibrations of the amide group in chitosan. Subsequently, the absorption peaks at 2944 cm^{-1}, 2851 cm^{-}

^{1}, 2943 cm^{-1}, and 2942 cm^{-1} correspond to the stretching of the C-H bond of GA in the hydrogels. The absorption band intensity between 3600 cm^{-1} and 3262 cm^{-1} is attributed to the O-H and N-H groups of PVA and PANi, which is most pronounced at the highest concentration of GA (0.48 wt.%), indicating an increase in intensity due to the functional group in this range. The incorporation of PANi into PVA-CS hydrogel with a higher GA concentration is suitable for light absorbers, as evidenced by the reduction in O-H group intensity with increasing GA content.

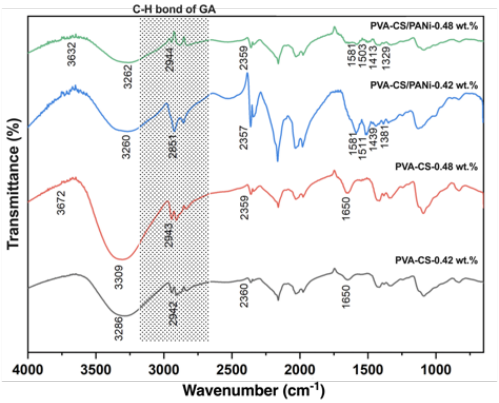

Fig. 1. FTIR Spectrum of dried PVA-CS hydrogel and PVA-CS/PANi with GA concentrations of 0.42 wt.% and 0.48 wt.%.

3.2 SEM Morphology Analysis of PVA-CS hydrogel and PVA-CS/PANi hydrogel

SEM analysis was conducted to investigate the surface morphology of PVA-CS hydrogel with various GA concentrations (0.42 wt.% and 0.48 wt.%) and for PVA-CS hydrogel with the incorporation of PANi. Fig. 2 (a-d) and Fig. 3 (a-d) depict the SEM morphology of the cross-section of the hydrogel with different magnifications. Fig. 2 (a-b) shows the interconnected micron-channel structure, which remains constant throughout, with varying GA concentrations. The consistent distribution of pores with diameters of several microns across the PANi-containing hydrogel indicates homogeneous gelation in the hydrogel[23]. In contrast, as depicted in Figs. 2(c-d), the microporous pore size decreases with an increase in GA concentration in the absence of PANi, and the structure distribution is inconsistent across the hydrogel. Furthermore, Fig. 3 shows a high-magnification image of the wrinkled internal surface for both types of hydrogels. The wall structure of the wrinkled internal surface is an indicator of shrinkage of the polymeric skeleton of the PVA network during the dehydration of the hydrogel [24]. Fig. 3(b) shows the visible wrinkled internal surface in the hydrogel with a 0.48 wt.% GA concentration incorporated into PANi, indicating that the hydrogel can deliver a rapid water rate to the surface, which is crucial for the design of the SVG system. A hydrogel composed of many wrinkles can deliver rapid water loss even during drying at room temperature [25]. In contrast, Fig. 3 (d) hydrogel with the same GA concentration without PANi, where the hydrogel almost has no visibility of the internal wrinkle surface. However, as seen in Fig. 3(b), the absence of visible wrinkles on the surface of PVA-CS/PANi containing 0.42 wt.% of GA is associated with the hydrogel surface depicted in Fig. 2(b), where the hydrogel exhibited an uneven, nonporous structure.

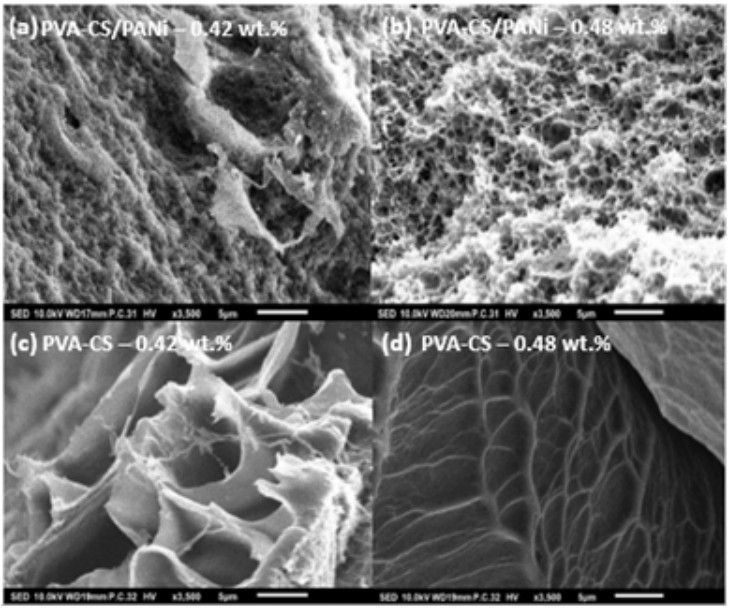

Fig. 2. Representative SEM image for the surface of micron channels (a-b) PVA-CS hydrogel with PANi of 0.42 wt.% and 0.48 wt.%; (c-d) and PVA-CS hydrogel of 0.42 wt.% and 0.48 wt.%

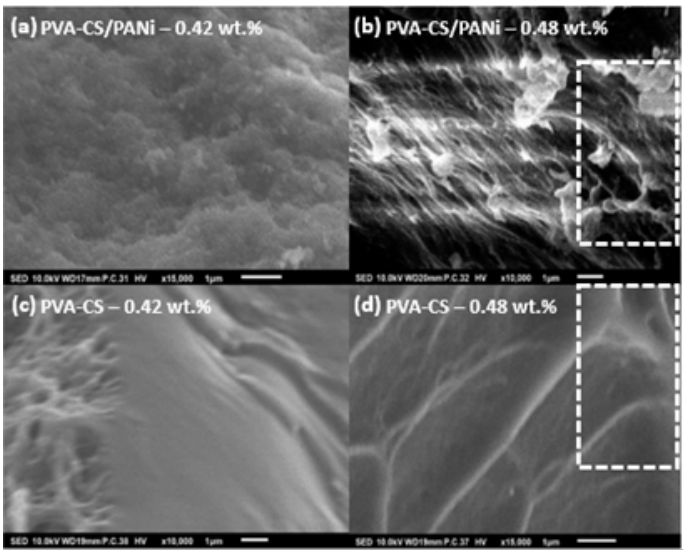

Fig. 3. Representative SEM images of the surface of wrinkled internal surface (a-b) PVA-CS hydrogel with PANi at 0.42 wt.% and 0.48 wt.%; (c-d) PVA-CS hydrogel at 0.42 wt.% and 0.48 wt.%.

3.3 Dynamic Rheology Analysis of PVA-CS hydrogel and PVA-CS/PANi hydrogel

Dynamic rheological studies were conducted on gel samples to evaluate the PVA-CS hydrogel and PVA-CS/PANi hydrogels with varying GA concentrations, focusing on crosslinking density and consistency modulus. Each sample was tested in a rheometer at a constant strain of 1% and a frequency of 1 Hz, corresponding to the linear viscoelastic range of the gel. Here, G′ and G′′ represent the elastic (storage modulus) and viscous (loss modulus) responses, respectively. As shown in Figs. 4(a) and 4(b), the dynamic frequency-sweep experiments on the gels reveal a wide linear viscoelastic region. In each instance, the storage modulus is greater than the loss modulus, indicating the

polymeric skeleton. The results demonstrate that the inclusion of PANi into the PVA and chitosan network structure, such structure is significant for energy dissipation. The relative modulus enhancement is greater for PVA-CS hydrogels with PANi and the remarkable modulus (G') was obtained by PVA-CS hydrogels with 0.48 wt.% of GA. The non-covalent association between the PVA-CS phase with PANi in the system contributes to the enhancement of the modulus value. The lower value of the loss modulus indicates an effective restriction of the polymer chain [26]. The significant reaction of PANi with the hydrogels, which have the same GA content of 0.48 wt.%, is evident in Fig. 4(b) and (d); as the frequency increases, the storage modulus value also increases. The higher value of storage modulus indicates a stronger mechanical strength of the hydrogel [23]. Furthermore, based on Figs. 4 (c) and 4 (d), showing the strain amplitude, the storage modulus was found to be larger than the loss modulus within a relatively small strain amplitude; this indicates that the rheological behaviour in this region is dominated by an elastic, rather than a viscous, property. This also indicates the reaction forming between polymer chains and crosslinkers. Hydrogels with PANi incorporation show an increase in the storage modulus with the increased value of GA concentrations; from this observation, the PANi incorporation with respect to the GA concentrations produced a consistent value of storage modulus if compared to that of the PVA-CS hydrogel, which had an inconsistent elastic modulus. However, viscous behaviour became superior to elastic behaviour as the strain amplitude gradually increased because the storage modulus decreased more rapidly after the breaking point (Table 1) than the loss modulus with increasing strain amplitude. This finding indicates that elastic stresses are relaxed and converted into viscous stresses by the microstructural arrangement.

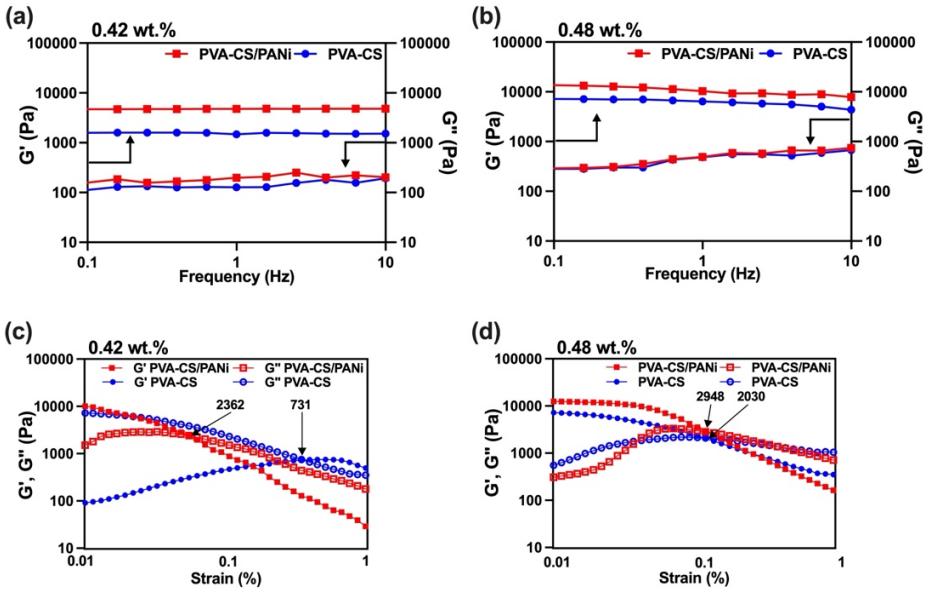

Fig. 4. Rheology studies for PVA-CS hydrogel and PVA-CS hydrogel with PANi;
(a-b) Frequency-sweep data of 0.42 wt.% and 0.48 wt.%;
(c-d) Strain amplitude data of 0.42 wt.% and 0.48 wt.%.

Table 1
Storage modulus and loss modulus values for PVA-CS and PVA-CS/PANi with different GA concentrations

Frequency				
GA concentration	PVA-CS hydrogel with PANi		PVA-CS hydrogel	
	Storage Modulus (G´) (Pa)	Loss Modulus (G´´) (Pa)	Storage Modulus (G´) (Pa)	Loss Modulus (G´´) (Pa)
0.42 wt.%	4762.60	197.45	1475.60	127.48
0.48 wt.%	10322	491.88	6380.60	483.90
Strain				
GA concentration	PVA-CS hydrogel with PANi		PVA-CS hydrogel	
	Breaking point (Pa)		Breaking point (Pa)	
0.42 wt.%	2362		731	
0.48 wt.%	2948		2030	

3.4 Solar Vapor Generation Efficiency

The SVG efficiency of PVA-CS hydrogel and PVA-CS/PANi with 0.42 wt.% and 0.48 wt.% of GA concentration were obtained from an outdoor experiment under an illumination intensity of 1 kW/m^2 for 1 hour. The initial and after weight of water and the initial and after temperature were taken before and after conducting the experiment in order to utilize the frequently used equation of solar vapor efficiency that is $\eta=\Delta m \times h_{LV} / P_{in}$ as shown in Tables 2 and 3. Each hydrogel was placed in a small beaker with cotton floating between the bulk water and the hydrogel, as the obtained hydrogels are not buoyant at the water's surface. Due to the penetration of PANi into the PVA-CS hydrogel structure, a visible change in the hydrogel's colour from opaque to dark is an outcome of the hydrogel's porous structure, which results in a greater water transport rate through the hydrogel's pores as depicted in Fig. 6. Dark hydrogel is also more effective in absorbing sunlight as the water mass change increases particularly with higher GA concentration hydrogel as shown in Table 3. Indeed, the significance of these results lies in the difference between PVA-CS hydrogel and PVA-CS/PANi, with an 11% difference as shown in Fig. 5. The incorporation of PANi into the hydrogel improves its performance, facilitating enhanced SVG efficiency. The highest efficiency obtained (45.5%) for PVA–CS/PANi with 0.48 wt.% GA indicates a 34% improvement compared to the PVA–CS/PANi with 0.42 wt.% of GA. Although this value is below the 60–90% efficiency typically reported for high-performance polymer-based evaporators, it demonstrates a promising enhancement attributable to optimized crosslinking. This result suggests that further modifications, such as doping PANi or incorporating hybrid photothermal fillers, could enhance the SVG efficiency toward commercial viability.

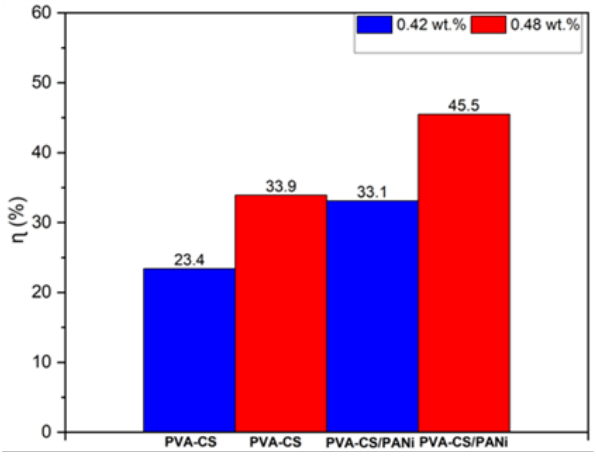

Fig. 5. SVG efficiency of PVA-CS hydrogel and PVA-CS/PANi

Table 2
Parameter of SVG efficiency of PVA-CS hydrogel

PVA-CS hydrogel	Water Mass Loss Rate ($kg\ m^{-2}h^{-1}$)	Average Water Temperature Difference (°C)	Sensible Heat ($kJ\ kg^{-1}$)	Latent Heat ($kJ\ kg^{-1}$)	η (%)
0.42 wt.%	0.3654	11	45.98	2257	23.4
0.48 wt.%	0.5293	12	50.16		33.9

Table 3
Parameter of SVG efficiency of PVA-CS hydrogel with PANi

PVA-CS/PANi hydrogel	Water Mass Loss Rate ($kg\ m^{-2}h^{-1}$)	Average Water Temperature Difference (°C)	Sensible Heat ($kJ\ kg^{-1}$)	Latent Heat ($kJ\ kg^{-1}$)	η (%)
0.42 wt.%	0.5169	11	45.98	2257	33.1
0.48 wt.%	0.7115	11	45.98		45.5

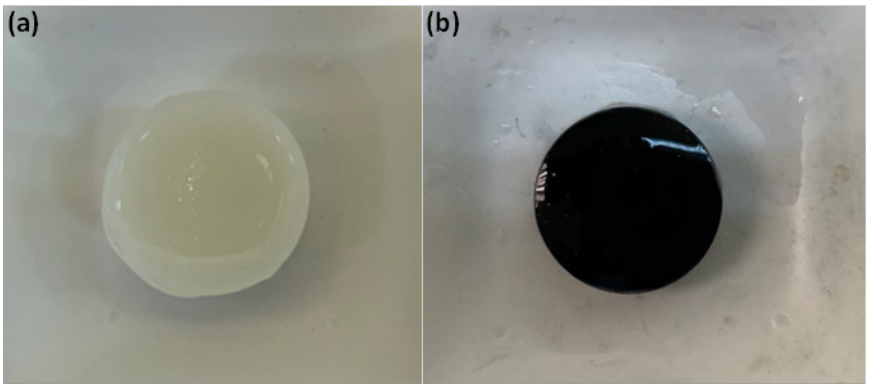

Fig. 6. Gel images of PVA-CS hydrogel and PVA-CS/PANi hydrogel.

4. Conclusions

The characterization analysis has revealed that, based on variable selection, the GA content of 0.48 wt.% is deemed suitable as the crosslinker for the PVA/Chitosan with PANi hydrogel study. This analysis can be justified by the SEM morphology and the internal wrinkles visible, which show a significant improvement when polyaniline is incorporated into the PVA/Chitosan hydrogel, consistent with the SVG system characteristics. From the FTIR spectra, the incorporation of Polyaniline into the PVA/Chitosan materials as a light absorber in the experiment is evidenced by a decrease in the O-H group absorption intensity, which is also proportional to the increasing of GA concentration. The rheology of hydrogels containing PANi exhibits an increase in the storage modulus with increasing GA concentration. Consequently, the incorporation of PANi at varying GA concentrations yields a consistent storage modulus. Besides, the enhancement of the storage modulus value suggests a synchronization of the GA content of 0.48 wt.% with the inclusion of PANi. The highest efficiency obtained for the PVA–CS/PANi hydrogel with 0.48 wt.% GA was 45.5%, corresponding to a water evaporation rate of approximately 0.71 kg m^{-2} h^{-1} under 1 sun illumination. This represents a 34% improvement over PVA–CS hydrogel (33.9%). It demonstrates that optimizing GA concentration can effectively enhance mechanical robustness and improve light-to-heat conversion performance. The improvement trend suggests that higher crosslinking densities enhance internal microchannel integrity, leading to faster water transport and reduced structural collapse during continuous illumination. The achieved 45.5% efficiency at minimal GA loading confirms that GA-mediated structural tuning is a practical and scalable approach for designing hybrid polymer hydrogels for sustainable solar vapor generation. Its tunable mechanical stability and porosity, governed by GA concentration, make it suitable for integration into low-cost, eco-friendly water purification modules, contributing to the broader goal of sustainable water resource management in off-grid or arid regions.

Acknowledgement

This research was funded by the UMP-IIUM-UiTM Sustainable Research Collaboration (SRCG) from Universiti Teknologi Mara and International Islamic University Malaysia, denoted as SRCG20-044-0044/100-TNCPI (1/1). The authors also would like to express an appreciation to Majlis Amanah Rakyat (MARA) for their technical and financial support.

References

[1] Mishra, R.K., *Fresh water availability and its global challenge.* British Journal of Multidisciplinary and Advanced Studies, 2023. **4**(3): p. 1-78.

[2] Zhang, P., et al., *Boosting the viable water harvesting in solar vapor generation: from interfacial engineering to devices design.* Advanced Materials, 2024. **36**(5): p. 2303976.

[3] Liu, B., et al., *The route for applied interfacial solar vapor generation: fundamental principles, device design, and practical application.* Energy & Environmental Science, 2025.

[4] Rather, R.A., M.A. Bhat, and A.H. Shalla, *An insight into synthetic and physiological aspects of superabsorbent hydrogels based on carbohydrate type polymers for various applications: a review.* Carbohydrate Polymer Technologies and Applications, 2022. **3**: p. 100202.

[5] Meera, B., et al., *Sustainable sponge-like composite hydrogel evaporator for highly efficient solar steam generation.* Materials Today Sustainability, 2023. **23**: p. 100439.

[6] Zou, H., et al., *Conjugated Polymer Hydrogel: A Highly Efficient Material of Solar Water Purification.* Journal of Polymer Materials, 2025. **42**(2).

[7] Serati, F., et al., *Solar-Driven Water Purification: Advancing PVA-Chitosan/PANI Hydrogel to Enhance Solar Vapor Generation for Freshwater Treatment.* IIUM Engineering Journal, 2025. **26**(1): p. 450-465.

[8] Guo, R., et al., *Porous and Salt-Tolerant Polyelectrolyte Hydrogels for Excellent Solar Evaporation.* Industrial & Engineering Chemistry Research, 2025. **64**(3): p. 1849-1858.

[9] Liu, H., et al., *Gradient-Charged Hydrogels for Highly Efficient Solar Steam Generation and Desalination.* Langmuir, 2023. **39**(38): p. 13641-13648.
[10] Hao, S., et al., *Fabrication of chitosan-based hydrogel embedded with antibacterial AgMXene nanocomposites as photothermal centers for solar steam generation and purification.* ACS Applied Energy Materials, 2024. **7**(3): p. 1250-1260.
[11] Zhu, M., et al., *Dome-arrayed chitosan/PVA hydrogel-based solar evaporator for steam generation, Sci Rep. 12 (2022) 4403*.
[12] Zhao, Q., et al., *Galactomannan/graphene oxide/Fe3O4 hydrogel evaporator for solar water evaporation for synergistic photothermal power generation.* Desalination, 2024. **570**: p. 117064.
[13] Zhang, R., et al., *Ultrastretchable, Tough, and Notch-Insensitive Hydrogels Formed with Spherical Polymer Brush Crosslinker.* Macromolecular Rapid Communications, 2017. **38**(22): p. 1700455.
[14] Nicol, E., et al., *Photo-cross-linked self-assembled poly (ethylene oxide)-based hydrogels containing hybrid junctions with dynamic and permanent cross-links.* ACS Macro Letters, 2018. **7**(6): p. 683-687.
[15] Wang, Z.J., et al., *Azo-crosslinked double-network hydrogels enabling highly efficient mechanoradical generation.* Journal of the American Chemical Society, 2022. **144**(7): p. 3154-3161.
[16] Distantina, S., et al., *Preparation and characterization of glutaraldehyde-crosslinked kappa carrageenan hydrogel.* Engineering Journal, 2013. **17**(3): p. 57-66.
[17] Ritonga, H., et al. *Preparation of hydrogel chitosan co-polyacrilamide crosslinked glutaraldehyde*. in *1st International Conference on Science and Technology, ICOST 2019*. 2019. European Alliance for Innovation (EAI).
[18] Teixeira, M., et al., *Green optimization of glutaraldehyde vapor-based crosslinking on poly (vinyl alcohol)/cellulose acetate electrospun mats for applications as chronic wound dressings. Proceedings. 5 (2021)*.
[19] Matty, F.S., M.T. Sultan, and A.K. Amine, *Swelling behavior of cross-link PVA with glutaraldehyde.* Pure Appl. Sci. Ibn Al-Haitham J. Pure Appl. Sci, 2015. **28**: p. 136-146.
[20] Yan, S., et al., *Thermo-and pH-sensitive poly (vinylmethyl ether)/carboxymethylchitosan hydrogels crosslinked using electron beam irradiation or using glutaraldehyde as a crosslinker.* Polymer international, 2009. **58**(11): p. 1246-1251.
[21] Yue, Y., *Designing ultrahigh-water-content, tough, and crack-resistant hydrogels by balancing chemical cross-linking and physical entanglement.* ACS Applied Engineering Materials, 2024. **2**(3): p. 638-648.
[22] Nandiyanto, A.B.D., R. Oktiani, and R. Ragadhita, *How to read and interpret FTIR spectroscope of organic material.* Indonesian Journal of Science and Technology, 2019. **4**(1): p. 97-118.
[23] Zhao, L., et al., *A novel floatable composite hydrogel for solar evaporation enhancement.* Environmental Science: Water Research & Technology, 2020. **6**(1): p. 221-230.
[24] Mehrotra, T., et al., *Rapid immobilization of viable Bacillus pseudomycoides in polyvinyl alcohol/glutaraldehyde hydrogel for biological treatment of municipal wastewater.* Environmental Science and Pollution Research, 2020. **27**(9): p. 9167-9180.
[25] Yin, X., et al., *Macroporous double-network hydrogel for high-efficiency solar steam generation under 1 sun illumination.* ACS applied materials & interfaces, 2018. **10**(13): p. 10998-11007.
[26] Zhao, F., et al., *Highly efficient solar vapour generation via hierarchically nanostructured gels.* Nature nanotechnology, 2018. **13**(6): p. 489-495.
[27] Wang, H., Wen, H., Hu, B. *et al.* Facile approach to fabricate waterborne polyaniline nanocomposites with environmental benignity and high physical properties. *Sci Rep* **7**, 43694 (2017).